Int J Clin Exp Pathol 2025;18(4):130-147
www.ijcep.com /ISSN:1936-2625/IJCEP0162097

Original Article

Effects of naphthoquinone scaffold-derived compounds on head and neck squamous cell carcinoma based on network pharmacology and molecular docking

Yiheng Liao, Lin Qiu, Anqi Tao, Cuiying Li

Central Laboratory, Peking University School and Hospital of Stomatology and National Center for Stomatology and National Clinical Research Center for Oral Diseases and National Engineering Research Center of Oral Biomaterials and Digital Medical Devices, Beijing 100081, China

Received November 18, 2024; Accepted March 1, 2025; Epub April 15, 2025; Published April 30, 2025

Abstract: Objectives: This study aimed to analyze the effects of naphthoquinone scaffold-derived compounds on head and neck squamous cell carcinoma (HNSCC) using network pharmacology and molecular docking. Methods: We screened candidate compounds from the ASINEX database and evaluated their drug likeness and toxicity. They identified 80 compounds with naphthalenone structures, focusing on 1,4-naphthoquinone and 1,2-naphthoquinone scaffolds. The possible targets of these compounds were predicted using databases like SwissTargetPrediction and Similarity Ensemble Approach Database (SEA). Results: The common targets between the compounds and HNSCC were identified, yielding 65 overlapping targets. A protein-protein interaction (PPI) network was constructed, and 20 hub genes were identified based on centrality metrics. Gene ontology (GO) enrichment and Kyoto Encyclopedia of Genes and Genomes (KEGG) pathway analysis revealed that these compounds' protective effects against HNSCC are associated with cancer-related pathways, such as those in cancer and proteoglycans in cancer. Molecular docking was performed to evaluate the binding affinity between the compounds and hub genes. The results showed that the compounds had strong binding affinities with key targets like MET and TYK2, with binding energies < -5 kcal/mol. Conclusions: The study suggests that naphthoquinone derivatives could serve as novel chemotherapy agents for HNSCC, warranting further research for clinical application.

Keywords: Naphthoquinone, molecular docking, head and neck squamous cell carcinoma, network pharmacology, virtual screening

Introduction

Squamous cell carcinoma (HNSCC) is the most prevalent and significant pathologic type of malignant tumor occurring in the head and neck. In 2022, approximately 54,000 new cases of HNSCC were diagnosed in the United States, and it was the seventh most common cancer globally [1]. Around 60% of patients are diagnosed at a locally advanced stage [2]. The overwhelming majority of advanced HNSCC cannot be cured by a sole surgical treatment approach and often necessitate multidisciplinary combined diagnosis and treatment. Radiotherapy in combination with cisplatin is referred to as concurrent chemoradiotherapy. Platinum - based concurrent chemoradiotherapy plays a highly significant role in the treatment paradigm of HNSCC. Clinically, numerous high - risk patients and some patients who do not meet the surgical criteria opt for concurrent chemoradiotherapy, which has been a standard treatment modality during the past 30 years [3]. Nevertheless, concurrent chemoradiotherapy also has issues such as drug resistance, severe side effects, and relatively obvious short - term and long - term toxicities [4, 5]. At present, no new treatment modality has been able to replace this cisplatin - based concurrent chemoradiotherapy. We hope to seek compounds with lower toxicity to take the place of cisplatin in concurrent chemoradiotherapy. Natural products are an important source of rich drug diversity. Roughly estimated, half of the drugs marketed nowadays are derived from natural medicines, which may be an important

https://doi.org/10.62347/CMQJ5473

research direction for the development of low - toxicity drugs [6].

Naphthoquinone derivatives are a common class of natural compounds originating from marine fungi and plants [7, 8]. In theory, there are six possible naphthoquinones, but only three, namely 1,4-naphthoquinones, 1,2-naphthoquinones, and 2,6-naphthoquinones, can be stably synthesized. Among these, 1,4-naphthoquinone (ortho-naphthoquinone) is the most stable and common, while 1,2-naphthoquinone (meta-naphthoquinone) and 2,6-naphthoquinone are less common [9]. Naphthoquinone derivatives have been found to possess potential anticancer properties. Napabucasin (BBI-608), Sepantronium bromide (YM-155), and Menadione (vitamin K3) have demonstrated significant anticancer effects against metastatic colorectal cancer, lymphoma, and liver cancer, both as monotherapies and in combination with other anticancer agents [10]. Plumbagin, a natural compound extracted from *Plumbago zeylanica L.*, induced apoptosis in oral squamous cell carcinoma (OSCC) cells by suppressing tumor cell proliferation [11]. It also inhibited Nrf2-mediated signaling pathway in human tongue squamous cell carcinoma cells [12]. Sepantronium bromide (YM-155) is a survivin inhibitor with a naphthoquinone structure. It is a potent inhibitor of the growth of SCC9 cells, which express high levels of survivin, and can enhance apoptosis and autophagic cell death in HNSCC cells [13, 14]. β-Lapachone (clinical trial form ARQ761) is a natural naphthoquinone compound with a unique quinone structure. It can be catalyzed by NQO1 to produce reactive oxygen species (ROS), thereby exerting a cytotoxic effect on HNSCC cells [15]. Isoplumbagin (5-hydroxy-3-methyl-1,4-naphthoquinone) is a naturally occurring quinone from Lawsonia inermis and Plumbago europaea, exerting anticancer effects by regulating mitochondrial dynamics and function [16]. Borges and colleagues investigated the anticancer activity and molecular mechanisms of 16 chemically selective derivatives of 1,4-naphthoquinone derived compounds in an OSCC model. One of these compounds exhibited superior pharmacokinetic characteristics compared to cisplatin and doxorubicin, demonstrating high selectivity and good tolerability in animals [17]. Aryl diazonium naphthoquinone compounds can intercalate into DNA, thereby exerting anticancer effects. Zorzanelli and colleagues studied 26 aryl diazonium naphthoquinone compounds, and one of these compounds demonstrated pharmacologic characteristics within the ideal criteria for drug development [5].

This study uses network pharmacology and virtual screening techniques to identify novel naphthoquinone derivatives for the treatment of HNSCC.

Materials and methods

Collection and screening of naphthoquinone scaffold-derived compounds

The candidate compounds used for screening were sourced from the ASINEX database (http://www.asinex.com). Data were imported from the database into DataWarrior (download from https://openmolecules.org/datawarrior/) [18]. To broaden the scope of our search, we used the “Structure” function in the software to draw the structure of naphthalenone. We then excluded naphthalenone from the resulting compounds and extracted those compounds that had structures similar to those of 1,2-naphthoquinone, 1,4-naphthoquinone, and 2,6-naphthoquinone.

The prediction of drug-likeness and toxic criteria

The drug similarity was assessed using SwissADME (http://www.swissadme.ch/index.php) according to Lipinski’s rule of five: molecular weight (< 500 g/mol), Topological Polar Surface Area (TPSA) (< 140 $Å^2$), Moriguchi octanol-water partition coefficient (MLogP) (≤ 4.15), Hydrogen Bonding Acceptor (HBA) (< 10) and Hydrogen Bonding Donor (HBD) (≤ 5). Subsequently, the toxicity of the compounds was evaluated using the OSIRIS Property Explorer (https://www.organic-chemistry.org/prog/peo/), which includes mutagenicity, tumorigenicity, irritancy, and reproductive effects. The software predicts toxicological risks through four principles: quantitative structure - activity relationships (QSAR), quantitative structure - property relationships (QSPR), built - in toxicity rules, and comparisons with known toxic compounds. Only non-toxic compounds that passed all toxicity criteria were further evaluated. The software also provided a Drug-score based

on toxicity and solubility, with a threshold set at 0.5.

Naphthoquinone derivatives and common target prediction in HNSCC

Possible targets of 1,4-naphthoquinone scaffold-derived compounds were predicted using the SwissTargetPrediction Database (STP) (http://www.swisstargetprediction.ch/) and the Similarity Ensemble Approach Database (SEA) (https://sea.bkslab.org/) [19, 20]. Input the SMILES - format chemical formulas of compounds into the STP and SEA databases. STP constructs prediction models based on known compound - target interaction knowledge and conducts structural similarity comparisons between the input small molecules and a large number of compounds in the database. By using machine learning algorithms and statistical models and based on the target information of similar compounds, it predicts the potential targets of the input small molecules. SEA employs an integrated similarity method for prediction. It compares the input compound with multiple reference compounds in the database that have known target information, calculates the similarity scores between the input compound and the reference compounds, and comprehensively evaluates the possible targets of the input compound based on these scores and the target information of the reference compounds. Then, we removed duplicates from the targets obtained from the two databases.

We downloaded the differentially expressed genes in HNSCC from gene expression profiling interactive analysis (GEPIA) website [21]. Using the Venny website (https://bioinfogp.cnb.csic.es/tools/venny/index.html), we obtained a Venn diagram representing the common targets of naphthoquinone derivatives and HNSCC.

Construction of Protein-Protein Interaction (PPI) network and identification of key targets

We inputed the shared targets into the STRING platform (https://cn.string-db.org/) and used the multi-protein analysis function [22]. We imported the downloaded PPI data into Cytoscape 3.7.1 and visualized the PPI network [23]. We removed nodes that were not connected to the main network. Using the CytoNCA plugin, we filtered and selected 20 hub genes based on the criteria: Degree > 5, Betweenness > 20, and Closeness > 0.22 [24]. The PPI network was analyzed using the MCODE plugin for clustering. The criteria for clustering were set as follows: Node Score Cutoff = 0.2, K-Core = 2, and Max. Depth = 100.

Gene ontology (GO) enrichment analysis and Kyoto Encyclopedia of Genes and Genomes (KEGG) pathway analysis

We introduced the hub genes into the David platform (https://david.ncifcrf.gov/) [25]. We set the Identifier to “OFFICE_GENE_SYMBOL”, the species to “Homo sapiens”, and the List Type to “Gene List”, respectively. Then, select “GOTERM_BP_DIRECT”, “GOTERM_CC_DIRECT”, and “GOTERM_MF_DIRECT” in Gene Ontology, as well as “KEGG_PATHWAY” in Pathways. GO enrichment analysis and KEGG pathway analysis were conducted, and the results were visualized using R (4.4.1). Pathway diagrams were generated using the Pathview package [26].

Molecular docking

Molecular docking between the protein encoded by the hub gene and the compound was performed using AutoDock software. The 3D structure of the compound in SDF format was obtained from PubChem, and the SDF file was converted to pdbqt format using OpenBabel software. The structure of the target protein was downloaded from the PDB website (https://www.rcsb.org/) [27].

AutoDock Vina 1.1.2 was used for molecular docking to obtain the binding energy value, and the combination with the lowest binding energy was visually analyzed by PyMOL 2.4.0 software (http://www.pymol.org/pymol) [28]. Protein-ligand interaction profiler (PLIP) website was used to analyze the interaction forces between ligand and receptor (https://plip-tool.biotec.tu-dresden.de) [29].

Survival analysis in relation to core targets

Analysis of the overall survival in relation to 20 core targets was performed using the university of Alabama at Birmingham cancer data analysis portal (UALCAN) (http://ualcan.path.uab.edu/analysis.html) database [30]. This is a

Table 1. Physicochemical properties of the naphthoquinone scaffold-derived compounds

Compounds	Molecular weight	TPSA	MLogP	HBA	HBD	Bioavailability Score	Toxicity Mutagenic	Tumorigenic	Reproductive effective	Irritant	Durg-score	SAscore
1	295.29	93.53	1	5	0	0.55	None	None	None	None	0.84	3.03
2	307.34	57.61	1.28	3	1	0.55	None	None	None	None	0.58	2.31
3	243.26	46.61	0.29	3	0	0.55	None	None	None	None	0.51	2.27
4	354.81	83.14	-0.19	5	0	0.55	None	None	None	None	0.81	2.33
5	368.84	83.14	0.05	5	0	0.55	None	None	None	None	0.76	2.39
6	375.42	69.72	0.9	3	1	0.55	None	None	None	None	0.73	2.23
7	389.45	69.72	0.85	4	1	0.55	None	None	None	None	0.74	2.22
8	353.8	53.51	1.35	3	0	0.55	None	None	None	None	0.74	2.25

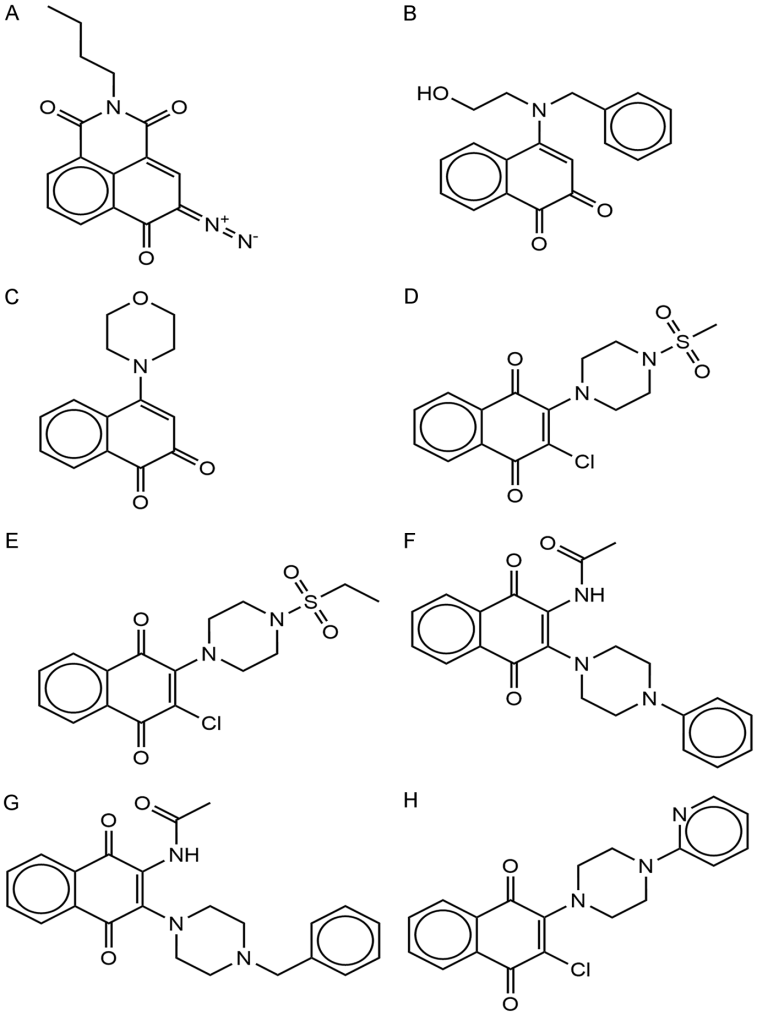

Figure 1. The eight compounds selected.

comprehensive and user - friendly online platform for cancer data analysis. It is mainly constructed based on the data from large - scale cancer research projects such as The Cancer Genome Atlas (TCGA) and Clinical Proteomic Tumor Analysis Consortium (CPTAC), and was used to mine and analyze cancer - related gene expression data, clinical information, and a variety of other cancer - related molecular features [31]. Kaplan-Meier method was used to analyze the relationship between hub genes expression and overall survival rate in HNSCC patients. *P* value < 0.05 was used for screening to indicate significance.

Prediction of synthesis routes and analysis of synthesis difficulty

Using Reaxys for retro-synthetic analysis to evaluate the synthesis difficulty and industrial production cost of potential chemotherapeutic drugs [32]. The synthesis route presented here is derived from published literature. Additionally, the software AiZynthFinder was utilized for retro-synthesis analysis. This tool combines Monte Carlo Tree Search (MCTS) with neural networks for retro-synthetic planning [33]. The R package Rdkit is used to calculate the synthetic accessibility score (SAscore) of compounds [34].

Results

Screening for drug-likeness and toxicity properties of naphthoquinone scaffold derivatives

We retrieved a comprehensive set of 575,302 compounds from the ASINEX database and screened them using DataWarrior chemical data analysis and visualization software V5.5.0. This process yielded 80 compounds with naphthalenone structures, including 26 compounds with a 1,4-naphthoquinone scaffold, 6 compounds with a 1,2-naphthoquinone scaffold, and no compounds with a 2,6-naphthoquinone scaffold. Additionally, we identified a compound substituted by two N_2 groups that, although not a naphthoquinone derivative, exhibited favorable drug-likeness with a Drug-score greater than 0.5. Therefore, we included this compound in subsequent studies. Nineteen 1,4-naphthoquinone and five 1,2-naphthoquinone compounds were predicted to have no toxicity properties (**Table 1**). A total of eight compounds with a Drug-score greater than 0.5 were selected (**Figure 1**).

Acquisition of common targets of naphthoquinone scaffold-derived compounds and HNSCC

Then, the targets related to the 8 compounds were retrieved from the STP (287) and SEA (283), respectively. After sorting out and removing duplicate targets, 508 targets were collect-

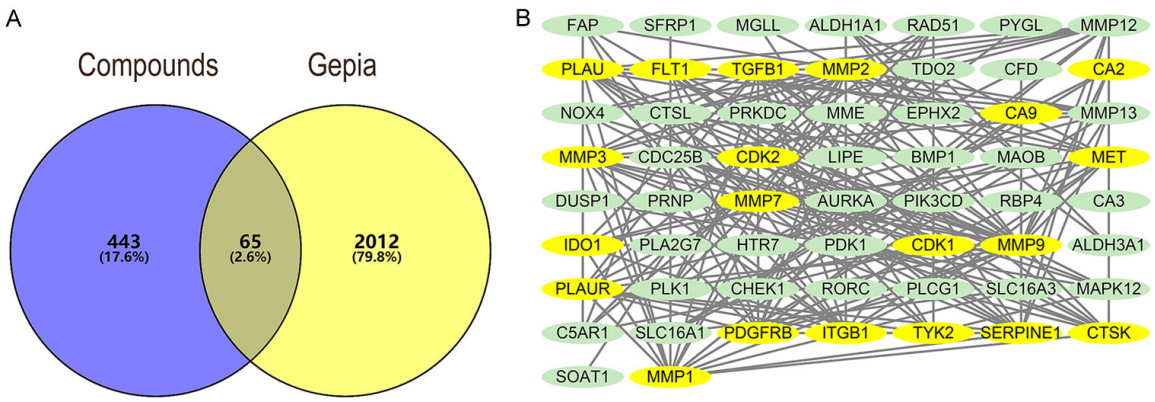

Figure 2. Compound targets and HNSCC targets. A: Venn diagram of predicted compound targets from the database and HNSCC differentially expressed genes downloaded from the Gepia website. B: PPI of the intersecting target genes, with hub genes represented by yellow nodes.

ed. The HNSCC differential expressed genes downloaded from the GEPIA website amounted to 2,077. The intersection of the two datasets yielded 65 overlapping targets (**Figure 2**).

Protein-protein interaction network analysis

We constructed a protein-protein interaction (PPI) network consisting of 65 targets. After removing nodes that were not connected to the main network, 58 nodes and 227 edges remained. We analyzed the network's topology using a series of metrics and identified 20 hub genes (**Table 2**). Proteins with high degree of centrality may interact with many other proteins; those with high betweenness centrality may act as bridges connecting different functional modules or protein groups; and those with high closeness centrality have a shorter average distance to other vertices, indicating a higher value. By integrating these centrality metrics, we can identify the most important proteins in the network, which hold the greatest research value.

Using the MCODE plugin in Cytoscape for clustering analysis, highly connected sub-networks were generated, and the targets were assigned to three clusters: Cluster 1 (12 nodes and 60 edges), Cluster 2 (8 nodes and 25 edges), and Cluster 3 (4 nodes and 5 edges) (**Figure 3**). It was found that 10 genes in Cluster 1 were hub genes. The nodes within each cluster were closely connected, while the connections between nodes of different clusters are sparse. GO analysis of the molecules in each cluster revealed that the corresponding biological processes (BPs) were primarily proteolysis, protein phosphorylation, and pyruvate catabolic process. The molecular functions (MFs) were mainly serine-type endopeptidase activity, ATP binding, and proton symporter activity for lactate. The cellular components (CCs) were mainly extracellular space, nucleoplasm, and lateral plasma membrane.

GO enrichment analysis, KEGG pathway analysis and construction of compound-target-pathway-disease network

To identify the top 10 target functions, GO enrichment analysis and KEGG pathway analyses were performed through the David database. Three categories of GO functional annotated targets were obtained.

BP was mainly associated with phosphorylation, positive regulation of cell migration, and proteolysis. CC was mainly associated with plasma membrane, extracellular region, and extracellular space. MF was mainly associated with protein binding, zinc ion binding, and serine-type endopeptidase (**Figure 4**).

There were 30 signaling pathways by KEGG analysis. We chose the top 10 signaling pathways presented in **Figure 4** and **Table 3**. The protective effects of naphthoquinone scaffold-derived compounds against HNSCC were closely linked to Pathways in cancer and Proteoglycans in cancer. The molecules in these two pathways might possess considerable research value.

Table 2. Gene names, degree value, betweenness centrality, and closeness centrality of key targets

Gene	Degree	Betweenness	Closeness
MMP9	28	1089.0054	0.6195652
TGFB1	22	295.60474	0.54285717
MMP2	20	109.318306	0.5135135
ITGB1	18	308.2275	0.5181818
SERPINE1	17	365.92612	0.5
PLAU	16	37.37246	0.47107437
MMP1	16	143.79555	0.4871795
MMP3	16	72.11424	0.49565217
MMP7	15	36.277256	0.475
PDGFRB	15	150.66086	0.48305085
PLAUR	14	42.858303	0.46721312
CTSK	12	61.80439	0.4453125
MMP12	12	6.0379367	0.4488189
MMP13	12	6.0379367	0.4488189
CDK2	12	307.97458	0.45238096
MET	12	75.3386	0.46721312
FLT1	11	40.20683	0.46341464
CTSL	10	7.7166667	0.41911766
CA9	9	164.92143	0.4488189
CDK1	9	174.11488	0.42857143
BMP1	8	0.52444446	0.4160584
IDO1	7	282.38104	0.46341464
PIK3CD	7	8.462358	0.40425533
TYK2	7	27.299515	0.40714285
PLK1	7	1.5587412	0.32947975
CHEK1	7	1.5587412	0.32947975
AURKA	7	41.521183	0.3607595
FAP	6	1.9669977	0.40140846
CA2	6	155.1567	0.4160584
CDC25B	6	7.3333335	0.32947975
RAD51	6	0.65874124	0.3275862
MAOB	6	226.16397	0.3607595
NOX4	5	0	0.42222223
PLCG1	5	3.0173738	0.37748346
PRKDC	5	0	0.3220339
MAPK12	5	134.22804	0.42222223
SLC16A3	5	30.905125	0.375
MME	5	9.126003	0.42222223
C5AR1	5	8.976191	0.40425533
ALDH1A1	5	276.54013	0.4488189
LIPE	4	151.6873	0.2923077
PDK1	4	37.307144	0.34756097
SLC16A1	4	4.1	0.33333334
TDO2	3	83.36645	0.34969324
CFD	3	150.99863	0.36305732
PLA2G7	3	112	0.39310345
EPHX2	3	110.33121	0.3275862
MGLL	2	12.766666	0.2614679
RBP4	2	0	0.34545454
ALDH3A1	2	6.75	0.27142859
RORC	1	0	0.35403726
SOAT1	1	0	0.2835821
SFRP1	1	0	0.32947975
PYGL	1	0	0.22709164
PRNP	1	0	0.3433735
HTR7	1	0	0.26635513
DUSP1	1	0	0.2984293
CA3	1	0	0.29533678

The KEGG pathways, Pathways in cancer, was visualized using Pathview (**Figure 5**). In addition, the network diagram of the relationship among compounds, key targets, top 10 signaling pathways, and HNSCC was also established (**Figure 6**).

Molecular docking

Molecular docking is utilized to evaluate the binding affinity between naphthoquinone framework drugs and their potential targets. The binding affinity is denoted by negative binding energy. Generally speaking, the binding energy between small molecules and proteins is ≤ -5.0 kcal/mol, indicating that the two have good binding activity [35]. The parameters for molecular docking were generated through the SwissDock (https://www.swissdock.ch/) website (**Table 4**).

It was found that the binding energies of all compounds and the 10 core genes were all < -5 kcal/mol. (**Figure 7**) Furthermore, among the core targets, MET had the strongest binding affinity with compound 7, with -10.3 kcal/mol. The binding affinity between TYK2 and compound 8 was the second strongest, being -10 kcal/mol (**Table 5**).

Hydrogen bonds are typically the strongest, followed by halogen bonds, while hydrophobic interactions are relatively weaker. Therefore, we have marked the locations of hydrogen bonds and halogen bonds in the figure (**Figure 8**).

Clinical relevance of core genes

Twenty hub genes were imported into the UALCAN database for clinical relevance analy-

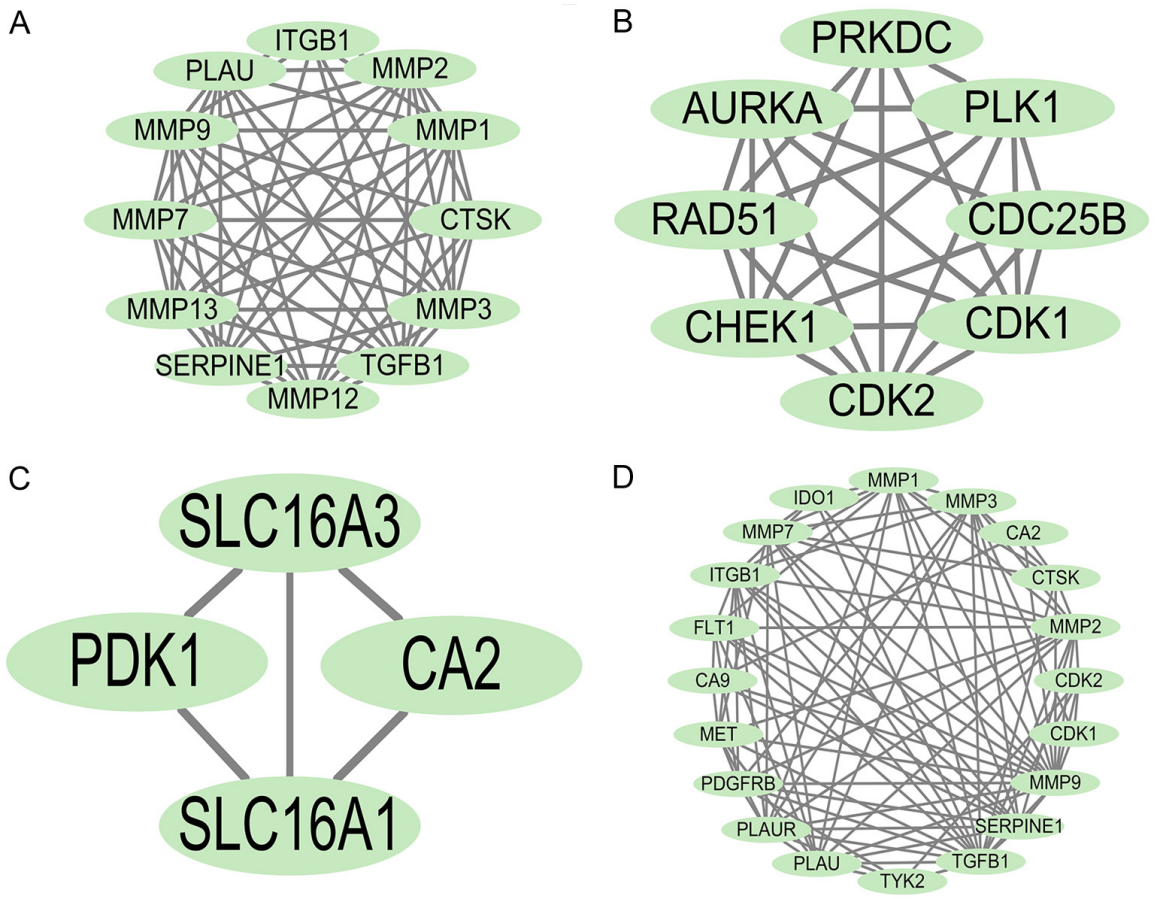

Figure 3. Topological analysis of the PPI. A: The first cluster obtained using the MCODE algorithm. B: The second cluster obtained using the MCODE algorithm. C: The third cluster obtained using the MCODE algorithm. D: PPI of hub genes.

sis. The expression levels of Plasminogen Activator, Urokinase (PLAU), and tyrosine kinase 2 (TYK2) was significantly correlated with overall survival ($P < 0.05$) related to overall survival of HNSCC patients (**Figure 9**). These two genes, serving as biological markers indicating tumor progression, may become new targets for drug development.

Prediction of synthesis routes and analysis of synthesis difficulty

The synthesis accessibility scores (SAscore) of the compounds was all lower than 5, indicating that the compounds were not difficult to synthesize. The compound 6, 7 and 8 had strong binding affinity with most hub genes, so we conducted retrosynthetic analysis on them (**Figure 10**).

Compound 6 did not have a synthesis route provided in Reaxys; therefore, we used AiZynthFinder for analysis. The results revealed that the synthesis route for compound 8 was identical to the one provided in Reaxys.

There were seven types of raw materials required for the synthesis of the compound. These molecules were all commercially available chemical reagents, and there are multiple methods for their synthesis. Among these methods, a synthesis route with lower cost and higher yield can be selected.

Discussion

The development of drugs, particularly anticancer drugs, is a lengthy process. We aim to expedite this process through network pharmacology and other data mining technologies. From 1981 to 2019, approximately 23.5% of newly approved drugs and 33.6% of approved small-molecule drugs worldwide were derived from natural products and their derivatives

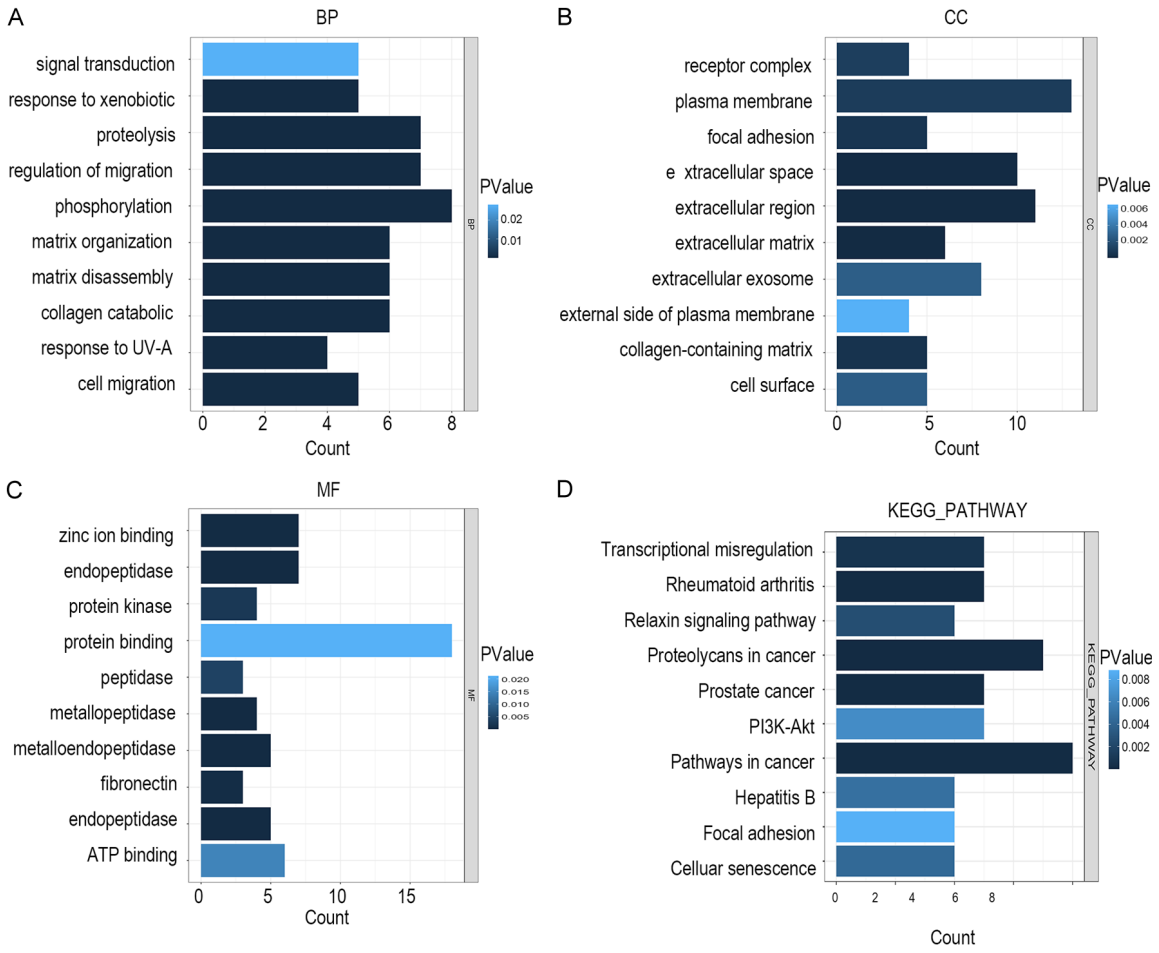

Figure 4. GO enrichment analysis, KEGG pathway analysis of hub genes. A: Biological processes of GO enrichment analysis. B: Molecular function of GO enrichment analysis. C: Cellular components of GO enrichment analysis. D: KEGG pathway analysis.

Table 3. Annotation of KEGG pathways with TOP10 enrichment degree and the involved potential targets

Term	Count	*P*-Value	Genes
Pathways in cancer	8	7.42E-05	PDGFRB, ITGB1, TGFB1, MMP1, MMP2, CDK2, MET, MMP9
Proteoglycans in cancer	7	2.96E-06	ITGB1, TGFB1, PLAU, MMP2, PLAUR, MET, MMP9
Rheumatoid arthritis	5	4.11E-05	TGFB1, FLT1, MMP1, CTSK, MMP3
Prostate cancer	5	4.84E-05	PDGFRB, PLAU, CDK2, MMP3, MMP9
Transcriptional misregulation in cancer	5	6.60E-04	FLT1, PLAU, MMP3, MET, MMP9
PI3K-Akt signaling pathway	5	0.006574962	PDGFRB, ITGB1, FLT1, CDK2, MET
Relaxin signaling pathway	4	0.002534665	TGFB1, MMP1, MMP2, MMP9
Cellular senescence	4	0.004321239	TGFB1, CDK2, SERPINE1, CDK1
Hepatitis B	4	0.004800012	TGFB1, CDK2, TYK2, MMP9
Focal adhesion	4	0.008813992	PDGFRB, ITGB1, FLT1, MET

[36]. Natural drugs can be categorized based on their sources into plant-based drugs, animal-derived drugs, mineral drugs, microbial drugs, fungal drugs, and marine organism drugs, encompassing a wide variety. Compared to large molecule drugs, small molecule drugs generally offer advantages such as better chemical stability, simpler storage condi-

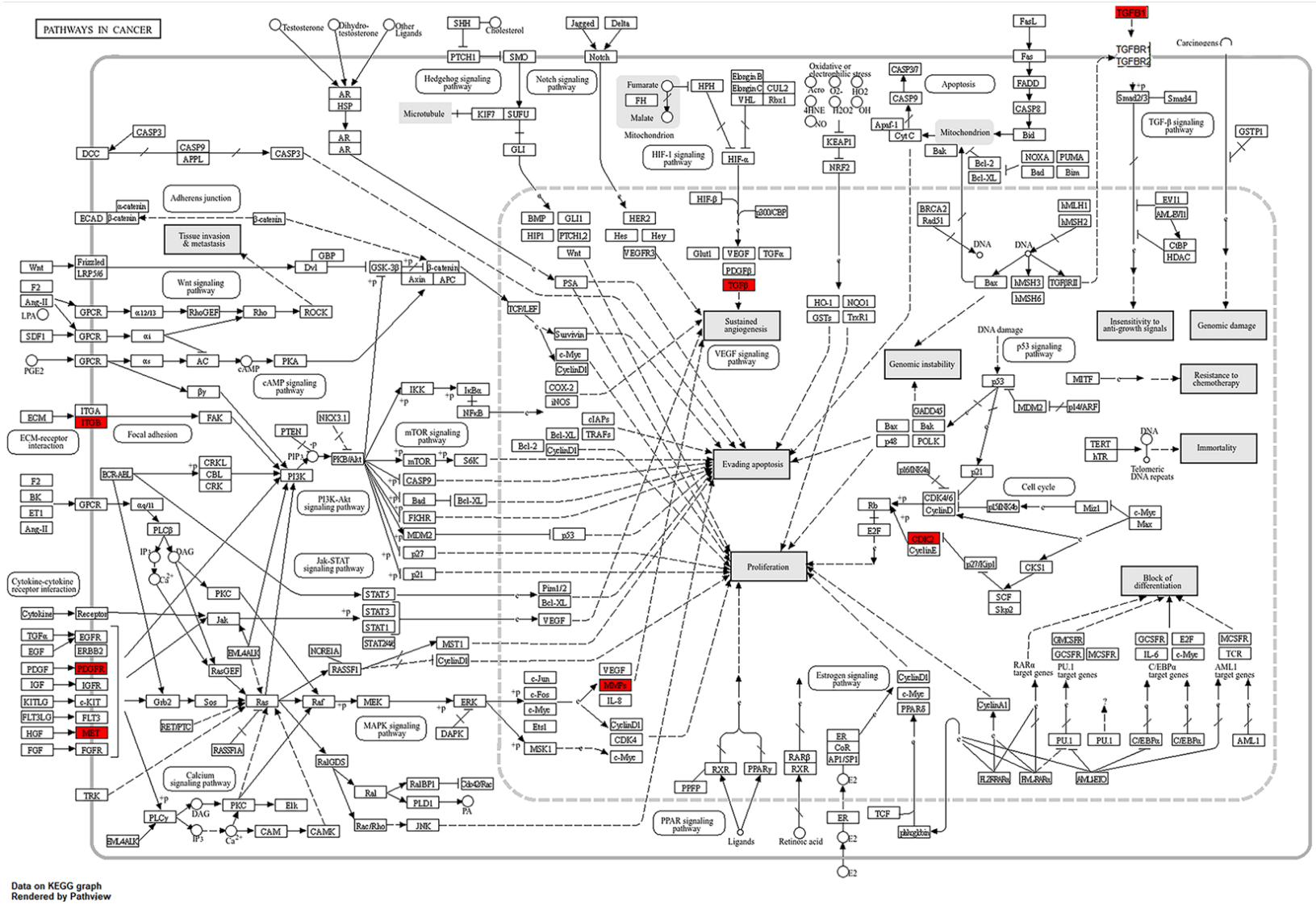

Figure 5. Topological structure diagram of Pathways in cancer.

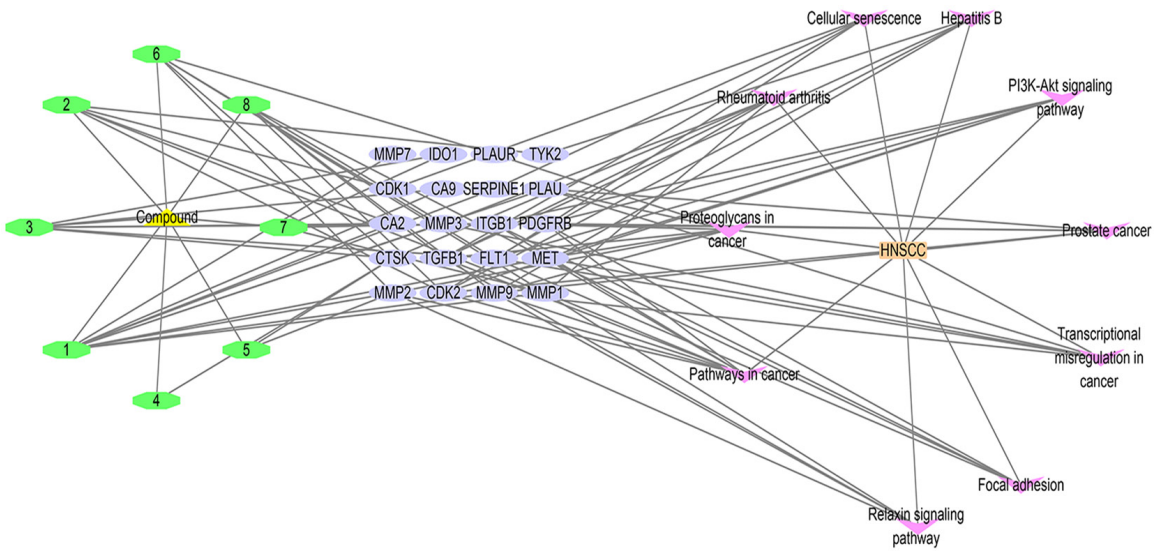

Figure 6. Compounds-target-pathway-disease network.

Table 4. Grid docking parameters in molecular docking

Target name	PDB ID	X center	Y center	Z center
PLAU	1C5W	16	4	17
PLAUR	1YWH	44	0	36
TYK2	3LXN	-10	3	17
MMP9	1GKC	55	20	129
TGFB1	1KLA	0	0	0
MMP2	1CK7	61	95	144
ITGB1	3G9W	27	1	-8
SERPINE1	1A7C	13	13	20
MMP1	1AYK	0	15	14
MMP3	1B3D	-4	28	17
MMP7	1MMP	22	38	43
PDGFRB	1GQ5	-7	28	4
CTSK	1ATK	-31	-23	63
CDK2	1AQ1	0	28	19
MET	1FYR	39	0	84
FLT1	1FLT	1	-2	24
CA9	2HKF	4	6	5
CDK1	4Y72	7	-53	193
IDO1	2D0T	66	33	21
CA2	12CA	-7	0	16

tions, a variety of oral administration routes, and relatively fewer side effects [37]. Small molecule drugs are a component of Antibody-Drug Conjugates (ADCs), some small molecule drugs target immune-related pathways and may complement antibody drugs, thereby enhancing the effectiveness of immunotherapy [38, 39]. Naphthoquinone compounds can penetrate cell membranes and may exert anticancer effects by mechanisms such as interfering with DNA replication in tumor cells and inhibiting their proliferation. The most widely documented isoform is known as 1,4-naphthoquinone. Various analogues have been discovered based on chemical modifications of 1,4-naphthoquinone, such as Juglone, Plumbagin, Shikonin, anthraquinone [40]. The naphthoquinone derivatives of interest in this study primarily originate from the ASINEX database. The ASINEX database is a comprehensive chemical database that focuses on providing high-quality compound libraries and drug development services.

Among the eight compounds we selected, all had structures that include 3-4 ring systems. The first three were derivatives of 1,2-naphthoquinone, while the remaining ones were derivatives of 1,4-naphthoquinone. Compound 3 contains a morpholine moiety. Morpholine derivatives are a class of anti-cancer agents that target various cancer cell lines, including breast cancer, gastric cancer, and non-small cell lung cancer [41, 42]. Morpholine contains a piperazine group, which can form amide bonds with other active groups. In this case, it forms a relatively stable carbon-nitrogen single bond with a benzene ring. Compounds 4, 5, 6, 7, and 8 all contained a piperazine structure.

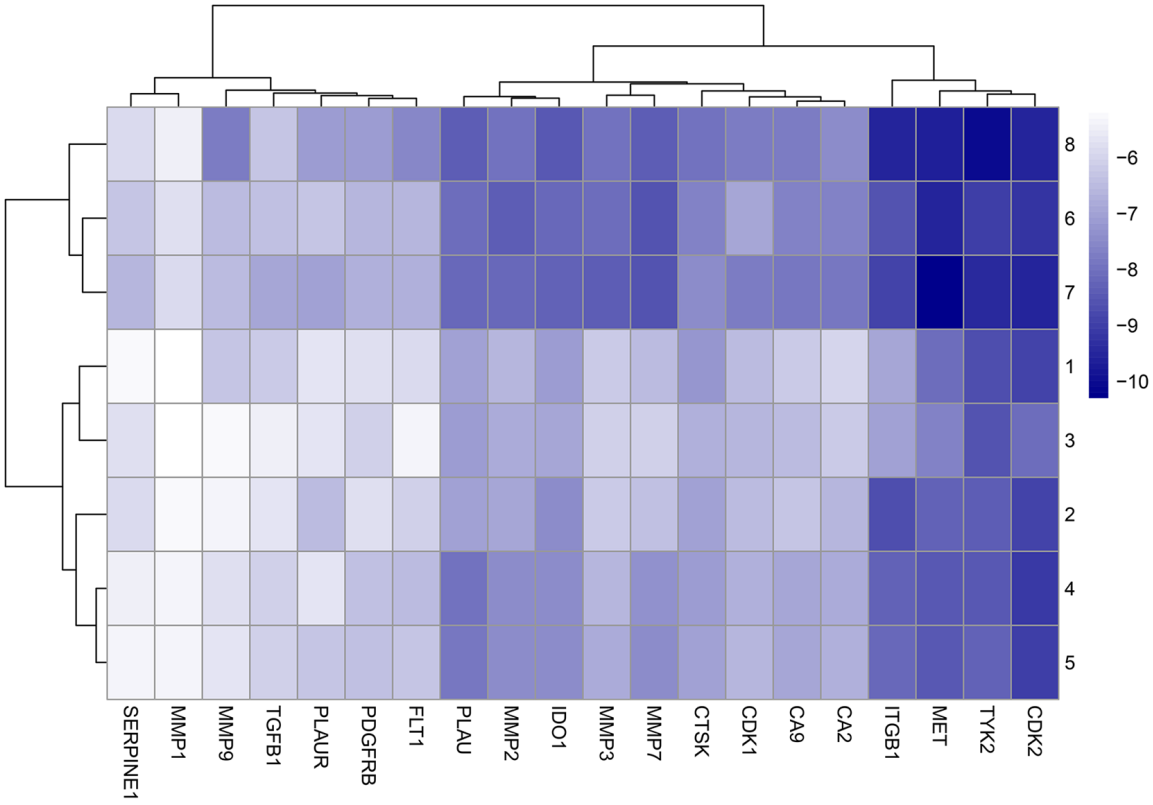

Figure 7. Molecular docking heat map of naphthoquinone scaffold-derived compounds and core targets.

Table 5. Molecular docking results between the naphthoquinone scaffold-derived compounds and hub targets

	1	2	3	4	5	6	7	8
PLAU	-7	-7	-7.1	-8	-7.9	-8.1	-8.2	-8.4
PLAUR	-5.7	-6.5	-5.7	-5.7	-6.3	-6.3	-7	-7.1
TYK2	-8.7	-8.4	-8.6	-8.5	-8.3	-9	-9.4	-10
MMP9	-6.3	-5.4	-5.3	-5.8	-5.7	-6.5	-6.5	-7.8
TGFB1	-6.2	-5.7	-5.5	-6.1	-6.1	-6.4	-6.9	-6.3
MMP2	-6.6	-6.9	-6.8	-7.4	-7.4	-8.4	-8.2	-8
ITGB1	-6.9	-8.7	-7	-8.3	-8.2	-8.6	-8.9	-9.5
SERPINE1	-5.3	-5.9	-5.8	-5.5	-5.4	-6.3	-6.6	-5.9
MMP1	-5.1	-5.3	-5.1	-5.4	-5.4	-5.8	-5.9	-5.5
MMP3	-6.2	-6.2	-6.1	-6.6	-6.8	-8.1	-8.4	-8
MMP7	-6.5	-6.4	-6.1	-7.3	-7.4	-8.6	-8.6	-8.4
PDGFRB	-5.8	-5.8	-6.1	-6.4	-6.4	-6.6	-6.7	-7.1
CTSK	-7.2	-7	-6.7	-7.1	-7	-7.6	-7.4	-8
CDK2	-8.9	-8.9	-8.1	-9.1	-9	-9.2	-9.5	-9.5
MET	-8.1	-8.3	-7.6	-8.5	-8.5	-9.5	-10.3	-9.6
FLT1	-5.9	-6.1	-5.4	-6.5	-6.3	-6.6	-6.7	-7.5
CA9	-6.2	-6.3	-6.5	-6.9	-6.9	-7.6	-7.9	-7.7
CDK1	-6.5	-6.5	-6.6	-6.7	-6.6	-6.9	-7.7	-7.7
IDO1	-7.1	-7.4	-6.9	-7.4	-7.4	-8.2	-8.3	-8.5
CA2	-6	-6.6	-6.2	-6.8	-6.7	-7.6	-7.9	-7.4

The data marked in red are the results of the molecular docking experiments for the compounds with the strongest binding force to proteins.

Compounds 4 and 5 had similar structures, both containing sulfonyl and piperazine groups. Piperazine derivatives have been extensively studied for their anticancer properties [43].

Compounds 6 and 7 were also quite similar; both were acetamides containing a benzylpiperazine. Natural products or their derivatives containing the piperazine structure, such as chrysin, monoflavonoid, gambogic acid, wogonin, and quercetin, exhibit certain cytotoxic effects on cancer cell lines [44]. Compound 8 contained a piperidine ring, which is widely present in pharmaceuticals, such as Chlorpromazine, Vandetanib, Delorazepam, and Lacosamide [45]. The antitumor activity of piperidine amide derivatives is remarkable [46, 47].

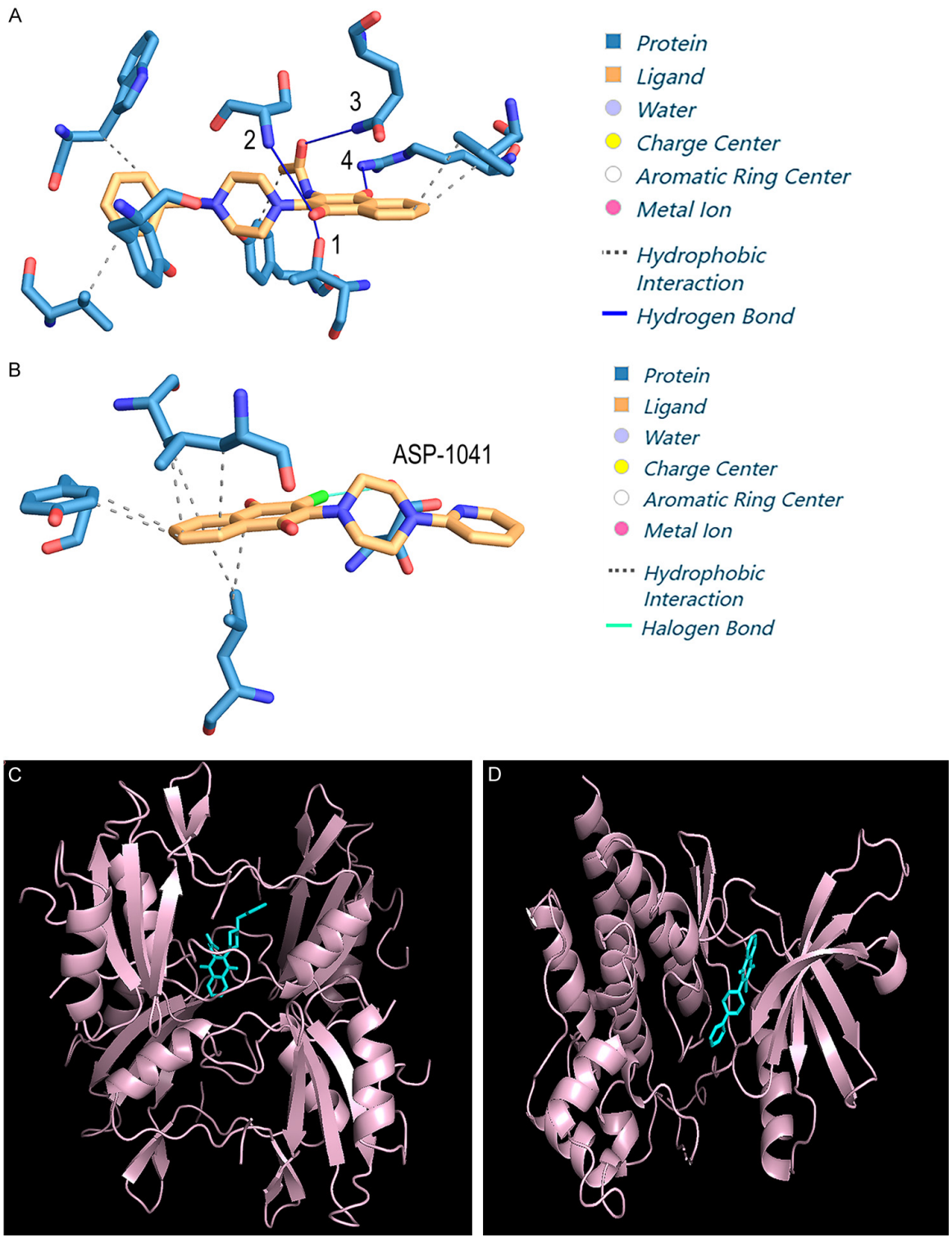

Figure 8. Molecular docking results between the compound and target. A: Analysis of protein-ligand interactions between compound 7 and MET. The numbers indicate the locations of the four hydrogen bonds, which are at THR-138, SER-139, GLN-145, and ARG-149, respectively. B: Analysis of protein-ligand interactions between compound 8 and TYK2. The image indicates the location of the halogen bonds. C: Three-dimensional molecular docking graph between compound 7 and MET. D: Three-dimensional molecular docking graph between compound 8 and TYK2.

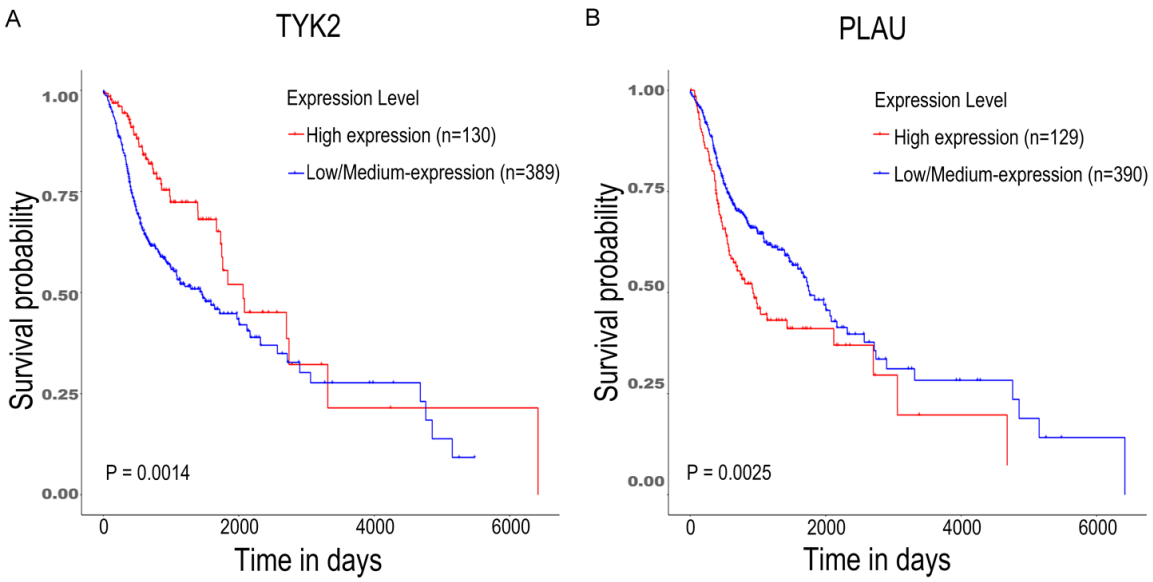

Figure 9. Overall survival analysis of core gene in the UALCAN database.

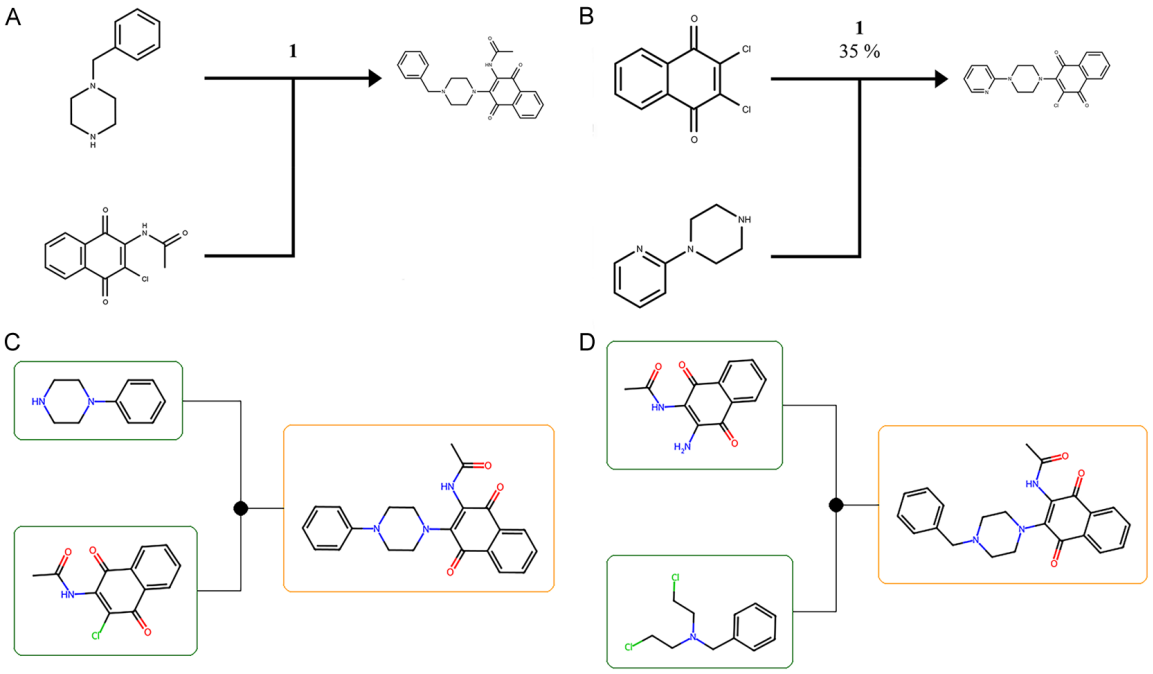

Figure 10. Final step of the synthetic route of compounds. A: Synthetic route of compound 7 from Reaxys. B: Synthetic route of compound 8 from Reaxys. C: Synthetic route of compound 6 from AiZynthFinder. D: Synthetic route of compound 7 from AiZynthFinder.

STP predicts the targets of compounds based on the similarity of their two-dimensional and three-dimensional structures to those of known compounds. Predictions can be made across three different species: human, rat, and mouse. The known compound-target interactions are sourced from the ChEMBL database, where the majority of targets are human proteins [48]. The SEA database integrates compound and target information from databases such as ChEMBL and MDDR (MDL Drug Data Report). It uses Daylight molecular fingerprints to calcu-

late the similarity of compounds and clusters the targets of similar compounds [49]. By combining data from these two databases, we can more comprehensively predict drug targets. The action of drugs on their targets is primarily determined by the structural compatibility of two molecules. For proteins, function is closely related to structure; therefore, the target proteins screened out may have connections in their signaling pathways. Small molecule drugs tend to have a broad spectrum of activity, so we set a larger range for identifying hub genes, namely 20.

Among these genes, only two were statistically significant in their relationship to the overall survival of HNSCC patients in the UALCAN database. However, other genes have also been reported in the literature to have carcinogenic effects. Therefore, the compounds' good binding characteristics to these genes are meaningful.

The 20 hub genes can be categorized into three main classes. The first - class genes have so far only undergone basic research and have not yet been involved in clinical trials, namely ITGB1, SERPINE1, CTSK, CDK2, CDK1, IDO1, and TYK2. The second-class consists of genes for which inhibitors have been developed and entered clinical trials but are not yet on the market; these are MMPs, TGFB1, PLAU, PDGFRB, PLAUR, FLT1, CA9, and CA2 [50]. The inhibitors of the third - class of genes have already been marketed. As a mature target, the focus should be on new drug development [51]. MET is a relatively mature drug target, and several MET inhibitors have passed clinical trials, including Capmatinib, Tepotinib, and Savolitinib [52].

Many genes are associated with cancer progression, but only a few can become drug targets. There are several reasons for this. Only a few genes are upstream driver genes. Some proteins lack clear binding pockets to accommodate drug molecules, while others may be difficult to target due to their location or functional characteristics. For example, transcription factors, which play a fundamental role in selective gene regulation within the cell nucleus, have a higher specificity in disease regulation compared to upstream signaling proteins such as kinases. However, due to the structural heterogeneity of transcription factors and their lack of active sites, they have traditionally been considered difficult to target with drugs. Research indicates that transcription factors exhibit highly dynamic protein - DNA and protein-protein interactions. The protein - DNA interaction interfaces are typically convex and positively charged, while the protein-protein interaction interfaces are usually flatter and lack binding pockets, making it challenging for small molecules to target them directly as drug targets [53]. Even if a specific gene is considered crucial for tumor growth, targeting it alone may have limited effects if there are alternative pathways within the same signaling cascade that can bypass this obstacle and continue to support the disease progression. Compared to oncogenes, tumor suppressor genes are more challenging to target with drugs. Additionally, cancer cells can resist drug effects through various mechanisms such as mutations and upregulation of compensatory signaling pathways. These factors make drug development an exceptionally challenging task [54].

Conclusion

This study combined network pharmacology and molecular docking to elucidate the molecular and pharmacological mechanisms by which naphthoquinone scaffold derivatives combat HNSCC. Further modifications of compounds 6, 7, and 8 may lead to the development of small - molecule chemotherapeutic drugs with clinical value, warranting further in-depth research.

Disclosure of conflict of interest

None.

Address correspondence to: Dr. Cuiying Li, Central Laboratory, Peking University School and Hospital of Stomatology, No. 22, Zhongguancun South Avenue, Haidian District, Beijing 100081, China. Tel: +86-17641602263; Fax: +86-17641602263; E-mail: kqlicuiying@bjmu.edu.cn

References

[1] Barsouk A, Aluru JS, Rawla P, Saginala K and Barsouk A. Epidemiology, risk factors, and prevention of head and neck squamous cell carcinoma. Med Sci (Basel) 2023; 11: 42.

[2] Lee YG, Kang EJ, Keam B, Choi JH, Kim JS, Park KU, Lee KE, Kwon JH, Lee KW, Kim MK, Ahn HK, Shin SH, Kim HR, Kim SB and Yun HJ. Treatment strategy and outcomes in locally ad-

vanced head and neck squamous cell carcinoma: a nationwide retrospective cohort study (KCSG HN13-01). BMC Cancer 2020; 20: 813.
[3] Argiris A, Karamouzis MV, Raben D and Ferris RL. Head and neck cancer. Lancet 2008; 371: 1695-1709.
[4] Crossman BE, Harmon RL, Kostecki KL, McDaniel NK, Iida M, Corday LW, Glitchev CE, Crow MT, Harris MA, Lin CY, Adams JM, Longhurst CA, Nickel KP, Ong IM, Alexandridis RA, Yu M, Yang DT, Hu R, Morris ZS, Hartig GK, Glazer TA, Ramisetty S, Kulkarni P, Salgia R, Kimple RJ, Bruce JY, Harari PM and Wheeler DL. From bench to bedside: a team's approach to multidisciplinary strategies to combat therapeutic resistance in head and neck squamous cell carcinoma. J Clin Med 2024; 13: 6036.
[5] Zorzanelli BC, Ouverney G, Pauli FP, da Fonseca ACC, de Almeida ECP, de Carvalho DG, Possik PA, Rabelo VW, Abreu PA, Pontes B, Ferreira VF, Forezi L, da Silva FC and Robbs BK. Pro-apoptotic antitumoral effect of novel acridine-core naphthoquinone compounds against oral squamous cell carcinoma. Molecules 2022; 27: 5148.
[6] Yang GX, Ma GL, Li H, Huang T, Xiong J and Hu JF. Advanced natural products chemistry research in China between 2015 and 2017. Chin J Nat Med 2018; 16: 881-906.
[7] Li Y, Yelv L, Wu X, Liu N and Zhu Y. Design, synthesis and biological evaluation of marine naphthoquinone-naphthol derivatives as potential anticancer agents. J Enzyme Inhib Med Chem 2024; 39: 2412865.
[8] Yen JH, Keak PY, Wu CL, Chen HJ, Gao WY, Liou JW, Chen YR, Lin LI and Chen PY. Shikonin, a natural naphthoquinone phytochemical, exerts anti-leukemia effects in human CBF-AML cell lines and zebrafish xenograft models. Biomed Pharmacother 2024; 179: 117395.
[9] Mancini I, Vigna J, Sighel D and Defant A. Hybrid molecules containing naphthoquinone and quinolinedione scaffolds as antineoplastic agents. Molecules 2022; 27: 4948.
[10] Angulo-Elizari E, Henriquez-Figuereo A, Morán-Serradilla C, Plano D and Sanmartín C. Unlocking the potential of 1,4-naphthoquinones: a comprehensive review of their anticancer properties. Eur J Med Chem 2024; 268: 116249.
[11] Chen PH, Lu HK, Renn TY, Chang TM, Lee CJ, Tsao YT, Chuang PK and Liu JF. Plumbagin induces reactive oxygen species and endoplasmic reticulum stress-related cell apoptosis in human oral squamous cell carcinoma. Anticancer Res 2024; 44: 1173-1182.
[12] Pan ST, Qin Y, Zhou ZW, He ZX, Zhang X, Yang T, Yang YX, Wang D, Zhou SF and Qiu JX. Plumbagin suppresses epithelial to mesenchymal transition and stemness via inhibiting Nrf2-mediated signaling pathway in human tongue squamous cell carcinoma cells. Drug Des Devel Ther 2015; 9: 5511-5551.
[13] Yan X and Su H. YM155 down-regulates survivin and induces P53 up-regulated modulator of apoptosis (PUMA)-dependent in oral squamous cell carcinoma cells. Med Sci Monit 2017; 23: 1963-1972.
[14] Zhang L, Zhang W, Wang YF, Liu B, Zhang WF, Zhao YF, Kulkarni AB and Sun ZJ. Dual induction of apoptotic and autophagic cell death by targeting survivin in head neck squamous cell carcinoma. Cell Death Dis 2015; 6: 1771.
[15] Lewis JE, Costantini F, Mims J, Chen X, Furdui CM, Boothman DA and Kemp ML. Genome-scale modeling of NADPH-driven β-lapachone sensitization in head and neck squamous cell carcinoma. Antioxid Redox Signal 2018; 29: 937-952.
[16] Tsao YC, Chang YJ, Wang CH and Chen L. Discovery of isoplumbagin as a novel NQO1 substrate and anti-cancer quinone. Int J Mol Sci 2020; 21: 4378.
[17] Borges AA, de Souza MP, da Fonseca ACC, Wermelinger GF, Ribeiro RCB, Amaral AAP, de Carvalho CJC, Abreu LS, de Queiroz LN, de Almeida ECP, Rabelo VW, Abreu PA, Pontes B, Ferreira VF, da Silva FC, Forezi LDSM and Robbs BK. Chemoselective synthesis of mannich adducts from 1,4-naphthoquinones and profile as autophagic inducers in oral squamous cell carcinoma. Molecules 2022; 28: 309.
[18] López-López E, Naveja JJ and Medina-Franco JL. DataWarrior: an evaluation of the open-source drug discovery tool. Expert Opin Drug Discov 2019; 14: 335-341.
[19] Daina A, Michielin O and Zoete V. SwissTargetPrediction: updated data and new features for efficient prediction of protein targets of small molecules. Nucleic Acids Res 2019; 47: 357-364.
[20] Gu S and Lai LH. Associating 197 Chinese herbal medicine with drug targets and diseases using the similarity ensemble approach. Acta Pharmacol Sin 2020; 41: 432-438.
[21] Tang Z, Li C, Kang B, Gao G, Li C and Zhang Z. GEPIA: a web server for cancer and normal gene expression profiling and interactive analyses. Nucleic Acids Res 2017; 45: 98-102.
[22] Szklarczyk D, Kirsch R, Koutrouli M, Nastou K, Mehryary F, Hachilif R, Gable AL, Fang T, Doncheva NT, Pyysalo S, Bork P, Jensen LJ and von Mering C. The STRING database in 2023: protein-protein association networks and functional enrichment analyses for any sequenced genome of interest. Nucleic Acids Res 2023; 51: 638-646.

[23] Otasek D, Morris JH, Bouças J, Pico AR and Demchak B. Cytoscape automation: empowering workflow-based network analysis. Genome Biol 2019; 20: 185.
[24] Tang Y, Li M, Wang J, Pan Y and Wu FX. CytoNCA: a cytoscape plugin for centrality analysis and evaluation of protein interaction networks. Biosystems 2015; 127: 67-72.
[25] Dennis G Jr, Sherman BT, Hosack DA, Yang J, Gao W, Lane HC and Lempicki RA. DAVID: database for annotation, visualization, and integrated discovery. Genome Biol 2003; 4: 3.
[26] Luo W, Pant G, Bhavnasi YK, Blanchard SG Jr and Brouwer C. Pathview web: user friendly pathway visualization and data integration. Nucleic Acids Res 2017; 45: 501-508.
[27] Burley SK, Bhikadiya C, Bi C, Bittrich S, Chao H, Chen L, Craig PA, Crichlow GV, Dalenberg K, Duarte JM, Dutta S, Fayazi M, Feng Z, Flatt JW, Ganesan SJ, Ghosh S, Goodsell DS, Green RK, Guranovic V, Henry J, Hudson BP, Khokhriakov I, Lawson CL, Liang Y, Lowe R, Peisach E, Persikova I, Piehl DW, Rose Y, Sali A, Segura J, Sekharan M, Shao C, Vallat B, Voigt M, Webb B, Westbrook JD, Whetstone S, Young JY, Zalevsky A and Zardecki C. RCSB protein data bank: tools for visualizing and understanding biological macromolecules in 3D. Protein Sci 2022; 31: 4482.
[28] Eberhardt J, Santos-Martins D, Tillack AF and Forli S. AutoDock vina 1.2.0: new docking methods, expanded force field, and python bindings. J Chem Inf Model 2021; 61: 3891-3898.
[29] Adasme MF, Linnemann KL, Bolz SN, Kaiser F, Salentin S, Haupt VJ and Schroeder M. PLIP 2021: expanding the scope of the protein-ligand interaction profiler to DNA and RNA. Nucleic Acids Res 2021; 49: 530-534.
[30] Chandrashekar DS, Karthikeyan SK, Korla PK, Patel H, Shovon AR, Athar M, Netto GJ, Qin ZS, Kumar S, Manne U, Creighton CJ and Varambally S. UALCAN: an update to the integrated cancer data analysis platform. Neoplasia 2022; 25: 18-27.
[31] Chandrashekar DS, Bashel B, Balasubramanya SAH, Creighton CJ, Ponce-Rodriguez I, Chakravarthi BVSK and Varambally S. UALCAN: a portal for facilitating tumor subgroup gene expression and survival analyses. Neoplasia 2017; 19: 649-658.
[32] Lawson AJ, Swienty-Busch J, Géoui T and Evans D. The making of reaxys - towards unobstructed access to relevant chemistry information. Acs Symposium 2014; 1164: 127-148.
[33] Genheden S, Thakkar A, Chadimová V, Reymond JL, Engkvist O and Bjerrum E. AiZynthFinder: a fast, robust and flexible open-source software for retrosynthetic planning. J Cheminform 2020; 12: 70.
[34] Ertl P and Schuffenhauer A. Estimation of synthetic accessibility score of drug-like molecules based on molecular complexity and fragment contributions. J Cheminform 2009; 1: 8.
[35] Vanommeslaeghe K, Hatcher E, Acharya C, Kundu S, Zhong S, Shim J, Darian E, Guvench O, Lopes P, Vorobyov I and Mackerell AD Jr. CHARMM general force field: a force field for drug-like molecules compatible with the CHARMM all-atom additive biological force fields. J Comput Chem 2010; 31: 671-690.
[36] Newman DJ and Cragg GM. Natural products as sources of new drugs over the nearly four decades from 01/1981 to 09/2019. J Nat Prod 2020; 83: 770-803.
[37] Ma YS, Xin R, Yang XL, Shi Y, Zhang DD, Wang HM, Wang PY, Liu JB, Chu KJ and Fu D. Paving the way for small-molecule drug discovery. Am J Transl Res 2021; 13: 853-870.
[38] Fu Z, Li S, Han S, Shi C and Zhang Y. Antibody drug conjugate: the "biological missile" for targeted cancer therapy. Signal Transduct Target Ther 2022; 7: 93.
[39] Offringa R, Kötzner L, Huck B and Urbahns K. The expanding role for small molecules in immuno-oncology. Nat Rev Drug Discov 2022; 21: 821-840.
[40] Qiu HY, Wang PF, Lin HY, Tang CY, Zhu HL and Yang YH. Naphthoquinones: a continuing source for discovery of therapeutic antineoplastic agents. Chem Biol Drug Des 2018; 91: 681-690.
[41] Dhahagani K, Mathan Kumar S, Chakkaravarthi G, Anitha K, Rajesh J, Ramu A and Rajagopal G. Synthesis and spectral characterization of Schiff base complexes of Cu(II), Co(II), Zn(II) and VO(IV) containing 4-(4-aminophenyl)morpholine derivatives: antimicrobial evaluation and anticancer studies. Spectrochim Acta A Mol Biomol Spectrosc 2014; 117: 87-94.
[42] Zhu W, Sun C, Xu S, Wu C, Wu J, Xu M, Zhao H, Chen L, Zeng W and Zheng P. Design, synthesis, anticancer activity and docking studies of novel 4-morpholino-7,8-dihydro-5H-thiopyrano[4,3-d]pyrimidine derivatives as mTOR inhibitors. Bioorg Med Chem 2014; 22: 6746-6754.
[43] Azevedo-Barbosa H, Dias DF, Franco LL, Hawkes JA and Carvalho DT. From antibacterial to antitumour agents: a brief review on the chemical and medicinal aspects of sulfonamides. Mini Rev Med Chem 2020; 20: 2052-2066.
[44] Zhang RH, Guo HY, Deng H, Li J and Quan ZS. Piperazine skeleton in the structural modification of natural products: a review. J Enzyme Inhib Med Chem 2021; 36: 1165-1197.

[45] Frolov NA and Vereshchagin AN. Piperidine derivatives: recent advances in synthesis and pharmacological applications. Int J Mol Sci 2023; 24: 2937.
[46] Tala SD, Ou TH, Lin YW, Tala KS, Chao SH, Wu MH, Tsai TH, Kakadiya R, Suman S, Chen CH, Lee TC and Su TL. Design and synthesis of potent antitumor water-soluble phenyl N-mustard-benzenealkylamide conjugates via a bioisostere approach. Eur J Med Chem 2014; 76: 155-169.
[47] Misra RN, Xiao HY, Kim KS, Lu S, Han WC, Barbosa SA, Hunt JT, Rawlins DB, Shan W, Ahmed SZ, Qian L, Chen BC, Zhao R, Bednarz MS, Kellar KA, Mulheron JG, Batorsky R, Roongta U, Kamath A, Marathe P, Ranadive SA, Sack JS, Tokarski JS, Pavletich NP, Lee FY, Webster KR and Kimball SD. N-(cycloalkylamino)acyl-2-aminothiazole inhibitors of cyclin-dependent kinase 2. N-[5-[[[5-(1,1-dimethylethyl)-2-oxazolyl]methyl]thio]-2-thiazolyl]-4-piperidinecarboxamide (BMS-387032), a highly efficacious and selective antitumor agent. J Med Chem 2004; 47: 1719-1728.
[48] Zdrazil B, Felix E, Hunter F, Manners EJ, Blackshaw J, Corbett S, de Veij M, Ioannidis H, Lopez DM, Mosquera JF, Magarinos MP, Bosc N, Arcila R, Kizilören T, Gaulton A, Bento AP, Adasme MF, Monecke P, Landrum GA and Leach AR. The ChEMBL Database in 2023: a drug discovery platform spanning multiple bioactivity data types and time periods. Nucleic Acids Res 2024; 52: 1180-1192.
[49] Keiser MJ, Roth BL, Armbruster BN, Ernsberger P, Irwin JJ and Shoichet BK. Relating protein pharmacology by ligand chemistry. Nat Biotechnol 2007; 25: 197-206.
[50] Rashid ZA and Bardaweel SK. Novel Matrix Metalloproteinase-9 (MMP-9) inhibitors in cancer treatment. Int J Mol Sci 2023; 24: 12133.
[51] Scott EC, Baines AC, Gong Y, Moore R Jr, Pamuk GE, Saber H, Subedee A, Thompson MD, Xiao W, Pazdur R, Rao VA, Schneider J and Beaver JA. Trends in the approval of cancer therapies by the FDA in the twenty-first century. Nat Rev Drug Discov 2023; 22: 625-640.
[52] Zhang Y, Shen L and Peng Z. Advances in MET tyrosine kinase inhibitors in gastric cancer. Cancer Biol Med 2024; 21: 484-498.
[53] Zhuang JJ, Liu Q, Wu DL and Tie L. Current strategies and progress for targeting the “undruggable” transcription factors. Acta Pharmacol Sin 2022; 43: 2474-2481.
[54] Wang F, Ruan DY and Xu RH. Challenges and opportunities in oncology drug development and clinical research in China. Cell 2024; 187: 1578-1583.